Efficient Manipulation of Nanoparticle-Bound DNA via Restriction Endonuclease

Wei Jie Qin and Lin Yue Lanry Yung*

Department of Chemical and Biomolecular Engineering, National University of Singapore, 10 Kent Ridge Crescent, Singapore 119260

Received May 27, 2006; Revised Manuscript Received August 3, 2006

As a programmable biopolymer, DNA has shown great potential in the fabrication and construction of nanometer-scale assemblies and devices. In this report, we described a strategy for efficient manipulation of gold nanoparticle-bound DNA using restriction endonuclease. The digestion efficiency of this restriction enzyme was studied by varying the surface coverage of stabilizer, the size of nanoparticles, as well as the distance between the nanoparticle surface and the enzyme-cutting site of particle-bound DNA. We found that the surface coverage of stabilizer is crucial for achieving high digestion efficiency. In addition, this stabilizer surface coverage can be tailored by varying the ion strength of the system. Based on the results of polyacrylamide gel electrophoresis and fluorescent study, a high digestion efficiency of 90+% for particle-bound DNA was achieved for the first time. This restriction enzyme manipulation can be considered as an additional level of control of the particle-bound DNA and is expected to be applied to manipulate more complicated nanostructures assembled by DNA.

Introduction

In recent years, metallic nanoparticles have been attracting considerable attention as ideal candidates for ultrasensitive biomolecule detection or nanometer-scale assembly.[1] Biomolecules, such as DNA, antigen−antibody, and enzymes, are being investigated as linker molecules for guiding the self-assembly of nanomaterials due to their specific recognition capability and biochemical functions.[2] The integration of nanoparticles with biomolecules is currently a focused topic and has led to numerous applications, such as biological and biomedical detections,[3,4] biosensors,[5] and nanoparticle-based molecular switches.[6] As a particularly promising candidate for programmed assembly of nanoparticles, DNA shows excellent physical and chemical properties and has been used extensively. Besides their unique sequence-specific binding property and mechanical rigidity, DNA molecules can be processed by a variety of enzymes, such as endonucleases, ligases, and polymerase, with the atomic level accuracy. This processibility allows a more efficient and precise manipulation of DNA and therefore opens up the possibility to produce monodisperse DNA molecules of precisely known size and chemical composition.[7]

Among these DNA-processing enzymes, restriction endonucleases that can recognize short specific DNA sequences and cleave the DNA[8] have received considerable attention over the past few years. He and co-workers[9] first reported using restriction endonuclease *Hin*f I to cleave double-stranded DNA molecules that connect gold nanoparticles to a gold film. Yun and co-workers[10] demonstrated the absence of conformational changes of nanoparticle-bound DNA by successfully performing the enzyme (methyltransferases and restriction endonuclease) manipulation of the gold nanoparticle−DNA conjugate dimers. Kanaras et al.[11] as well as Wang et al.[12] reported using restriction endonucleases to cleave DNA molecules heavily loaded on gold nanoparticles with 65% digestion efficiency. Despite these recent studies, high digestion efficiency of nanoparticle-bound DNA by restriction endonuclease has not been demonstrated yet. This high efficient control is important for application of these bioconjugates because the nanoparticles with homogeneous length of DNA are crucial in the application of nano-assemblies with high precision and medical diagnosis with high reproducibility.

Here, we reported a systematic study on the restriction endonuclease manipulation of gold nanoparticle-bound DNA, which could contribute to a better understanding of enzymatic manipulation of nanoparticle−biomolecule conjugates. The digestion reaction was carried out under various conditions, including (i) stabilizer surface coverage, (ii) distance between nanoparticle surface and enzyme-cutting site of particle-bound DNA, and (iii) size of nanoparticles. Digestion efficiency as high as 90%+, which is similar to free DNA digestion in solution, was achieved for the first time. The application of this enzyme manipulation would substantially enrich the tool-box for tailoring nanoparticle-bound DNA or more complicated DNA-induced nano-assemblies and lead to the fabrication of more accurate and complex nanostructures.

Materials and Methods

Materials. Hydrogen tetrachloroaurate(III) trihydrate, trisodium citrate dehydrate, tannic acid, 4,4′-(phenylphosphinidene) bis-(benzenesulfonic acid) (PPBS), dithiothreitol (DTT), TEMED (*N*,*N*,*N*′,*N*′-tetramethylethylenediamine), glycerol, TBE buffer (Tris-borate EDTA buffer), NaCl, and $MgCl_2$ were purchased from Sigma-Aldrich. The synthetic DNA was purchased from Integrated DNA Technologies (Figure 1). Restriction endonuclease *Eco*RV (500 000 unit/mL) and bovine serum albumin (BSA) were obtained from New England Biolabs. 30% acrylamide/bis solution (29:1) ammonium persulfate, bromophenol blue, and ethidium bromide were obtained from Bio-Rad Laboratories. Milli-Q water with resistance >18 MΩ/cm was used throughout the experiments.

Synthesis and Characterization of Gold Nanoparticles. Gold nanoparticles were synthesized by the reduction of hydrogen tetrachloroaurate(III) trihydrate by trisodium citrate dihydrate and tannic acid.[13]

* Corresponding author. E-mail: cheyly@nus.edu.sg.

10.1021/bm060517o CCC: $33.50
Published on Web 10/12/2006

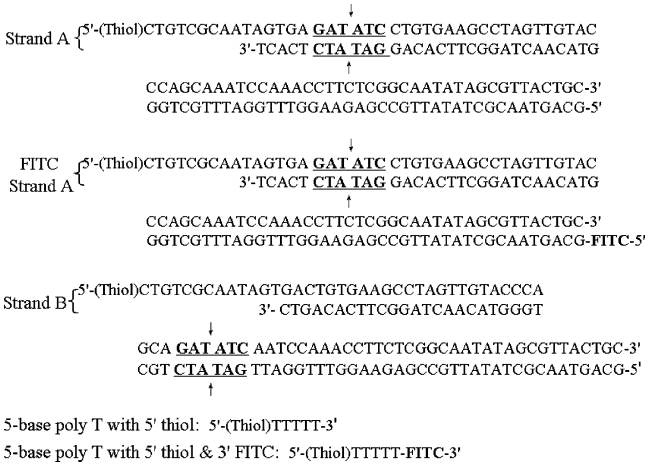

Figure 1. DNA sequences used in this study. Underlined sequences are the recognition site of *Eco*RV, and the arrows indicate the enzyme cleavage site.

To determine the size and size distribution of the resulting nanoparticles, TEM characterization was performed on a Philips CM300 FEG system operating at 200 kV. At least 200 particles were sized from TEM micrographs via graphics software "Image-Pro Express" (Media Cybernetics). Gold nanoparticles with mean diameters of 10 and 7 nm were used in this study.

Preparation of Nanoparticle−DNA Conjugates. Two complementary single-stranded DNAs (ssDNAs, sequences shown in Figure 1), one modified with a thiol linker, were mixed in equal molar amount in the hybridization buffer (50 mM Tris pH 8.0 and 50 mM NaCl). The mixture was briefly heated to 95 °C and then gradually cooled to room temperature to allow the formation of double-stranded DNA (dsDNA). The nanoparticle−DNA conjugates were prepared as previously described by Demers and co-workers[14] with modifications. Briefly, gold nanoparticles were incubated with 60 mM PPBS to gain necessary stability in mild salt concentration. Extra PPBS was removed by washing and centrifuging the samples with 50 mM Tris buffer (pH 8.0). Next, a 3× stoichiometric equivalence of 2 μM dsDNA was mixed with gold nanoparticles in 50 mM Tris buffer containing 50 mM NaCl. The samples were incubated at room temperature for 2 h, and 5′-thiolated TTTTT ssDNA (dT-ssDNA, Figure 1) was then added to the system followed by increasing the NaCl concentration to 100 mM. The final concentrations of nanoparticles and ssDNA were 90 nM and 45 μM, respectively. After 8 h of incubation, the NaCl concentration was gradually increased to 500 mM by adding a 5 M NaCl stock solution to the mixture in 6 h. The samples were incubated under this condition for an additional 24 h with intermittent vortex mixing. Finally, excess reagents were then removed by washing and centrifuging the samples with 50 mM Tris buffer three times. For conjugates without ssDNA, the dsDNA conjugation was stopped after 2 h of reaction by washing and centrifuging two times. Without ssDNA saturation, repeated washing and centrifuging may completely remove PPBS weakly adsorbed on nAu and cause nAu aggregation; thus the washing step was only performed two times.

Enzyme Manipulation of Nanoparticle-Bound DNA and Digestion Efficiency. The restriction endonuclease digestion of dsDNA was performed by incubating the conjugates with 100 units of *Eco*RV at 37 °C in a 200 μL reaction buffer for 20 h. After incubation, the enzyme was deactivated by adding 50 mM EDTA. The digested conjugates were characterized by polyacrylamide gel electrophoresis (PAGE). For PAGE characterization, the DNA residues were released from the nanoparticle surface by ligand exchange reaction with excess DTT. After the removal of the nanoparticles by centrifuging the samples at 13 000*g* for 15 min, the DNA solution was characterized by 12% PAGE (1X TBE as running buffer). The DNA bands were stained with ethidium bromide and captured by a UV/White Light gel documentation system (GeneGenius, Syngene). The enzyme digestion efficiency was calculated by dividing the amount of digested DNA fragments by the total amount of DNA in the same lane (digested + undigested). Each efficiency value reported was the average of three individual tests.

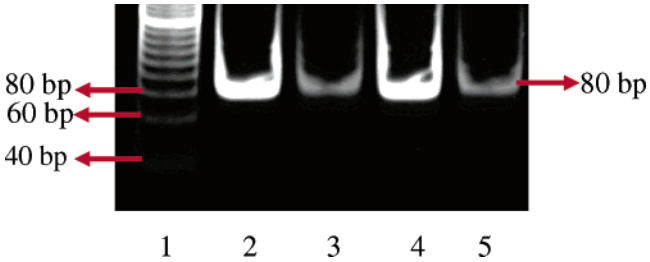

Figure 2. PAGE characterization of enzyme-digested 10 nm nAu-bound dsDNA without dT-ssDNA saturation. Lanes 1−5 correspond to: (1) 20 bp DNA ladder, (2) intact strand A without enzyme treatment, (3) enzyme-treated particle-bound strand A, (4) intact strand B without enzyme treatment, and (5) enzyme-treated particle-bound strand B.

Fluorescence Quantification of DNA Surface Coverage. The fluorescence measurement on dT-ssDNA surface coverage on nanoparticles was carried out with fluorescein thioisocyanate (FITC)-labeled DNA (Figure 1). The fluorescence measurement was performed using a luminescence spectrometer (Perkin-Elmer LS 50B) with a 1-cm cuvette. The samples were excited at 495 nm, and the emission spectra were recorded from 510 to 535 nm. All of the fluorescence measurements were carried out without the presence of the nanoparticles. For the dT-ssDNA surface coverage study, the FITC dT-ssDNA was released from nanoparticle by ligand exchange reaction with excess DTT. After overnight incubation with DTT at room temperature, the solutions containing displaced FITC dT-ssDNA were separated from the gold nanoparticles by centrifugation of the particle aggregates. The maximum fluorescent emission at 520 nm was converted to molar concentrations of the FITC dT-ssDNA by interpolation from a standard curve using known concentrations of FITC dT-ssDNA under exactly the same buffer condition and DTT concentration. Finally, the average surface coverage of FITC dT-ssDNA on nanoparticle was obtained by dividing the measured amount of dT-ssDNA by the actual amount of nanoparticle in the sample.

Results and Discussion

Importance of Short ssDNA Modification on the Surface of Gold Nanoparticles for Achieving High Enzyme Digestion Efficiency. In our experiments, it was found that the saturation of the nanoparticle surface with 5-base thiol-modified ssDNA (dT-ssDNA, Figure 1) is a necessary step to prevent nonspecific adsorption of restriction endonuclease on nanoparticles and to achieve high DNA digestion efficiency. When gold nanoparticle (nAu) without ssDNA modification was used, the enzyme digestion efficiency of the nAu-bound dsDNA was found to be 0%, even when a large amount of *Eco*RV was used. Figure 2 shows a 12% polyacrylamide gel image of 10 nm nAu bound with only dsDNA but without dT-ssDNA saturation after *Eco*RV digestion. As shown in the next section, if enzyme digestion occurs, DNA bands with lower molecular weight can be found on the gel. In Figure 2, however, no digested DNA band can be seen in lane 3 or lane 5, indicating that no digestion of particle-bound DNA was achieved with either strand A or strand B. This surprisingly low digestion efficiency is not likely due to the steric hindrance from nAu, because the enzyme recognition site of strand B is located in the middle of the DNA and is far away from nAu (43 bases away from the thiolated 5′ end). We attribute this low efficiency to two possible reasons: (1) Because of the high affinity of nucleotides to the gold surface[15,16] and low target dsDNA loading on nAu, the target dsDNA may

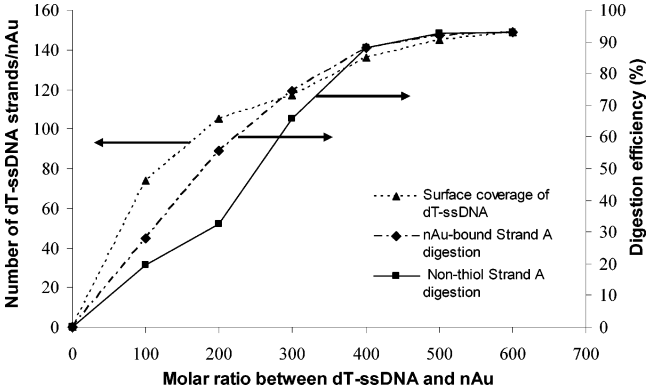

Figure 3. dT-ssDNA surface coverage on 10 nm nAu as well as corresponding enzyme digestion efficiency of particle-bound strand A and nonthiol strand A.

wrap around nAu[17] and impair its accessibility for enzyme binding and digestion; (2) the nonspecific adsorption of enzyme on the nAu surface may lead to a significant decrease of the free enzyme in the digestion system and, therefore, result in a severe drop in the digestion efficiency. This nonspecific adsorption of enzyme molecules on gold nanoparticles has been observed by other groups,[18] which causes protein denaturation and loss of biological functions.

To prevent or minimize the interaction between target dsDNA and nAu as well as enzyme adsorption, dT-ssDNA was used to saturate the nanoparticles surface prior to the enzyme treatment. dT was adopted because it has a much lower binding affinity with nAu surface and can lead to higher surface coverage.[16] Another advantage gained from this ssDNA surface saturation is the significant increase in the stability of nanoparticle. 10 nm nAu without this treatment may aggregate irreversibly in the digestion buffer required by the enzyme. However, the dT-ssDNA modification leads to a stronger steric repulsion among nAu particles, and thus no particle aggregation was observed even with the use of prolonged digestion time aiming to improve the digestion efficiency. Without dT-ssDNA saturation, the digestion of nAu-dsDNA shown above (Figure 2) could last for less than 8 h depending on the actual buffer condition.

Effect of ssDNA Surface Coverage on Enzyme Digestion Nanoparticle-Bound DNA. The dT-ssDNA surface coverage on nAu and its effect on enzyme digestion efficiency were studied using FITC-labeled dT-ssDNA (Figure 1). In our experiment, the fluorescent measurement was conducted after nAu removal by centrifugation because (1) the fluorescence signal of nAu-bound FITC dT-ssDNA can be quenched via the fluorescence resonance energy transfer (FRET) effect by nAu,[3,19] and (2) nAu has a maximum optical absorption at 520 nm, and their presence leads to a significant reduction of fluorescent signal by FITC dT-ssDNA whose emission maximum is also in the 520 nm range. Figure 3 shows the dT-ssDNA surface coverage on 10 nm nAu with different molar ratios of dT-ssDNA to nAu as well as the corresponding enzyme digestion efficiency. This ratio refers to the incubating molar ratio used during the incubation of the dT-ssDNA and nAu mixture for surface conjugation. The surface coverage of dT-ssDNA increases substantially with the increasing molar ratio of dT-ssDNA and nAu until a 400:1 ratio is reached, which results in a surface coverage of approximately 136 strands/particle (determined from fluorescent study using FITC-labeled dT-ssDNA). When the molar ratio goes beyond 400:1, there was only a minor increase in the surface coverage (less than 10%) as the molar ratio increased to 600:1. The saturation dT-ssDNA surface coverage obtained at a 600:1 molar ratio was found to be approximately

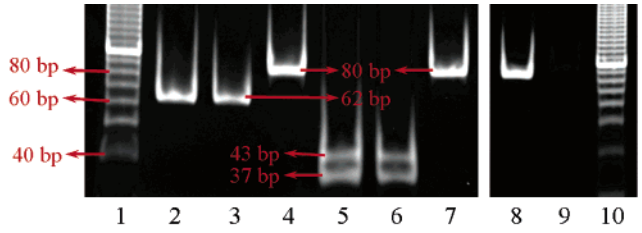

Figure 4. PAGE characterization of enzyme-digested 10 nm nAu-bound DNA. Lanes 1−7 correspond to: (1) 10 bp DNA ladder, (2) enzyme-digested particle-bound strand A, (3) enzyme-digested free strand A, (4) intact strand A without digestion, (5) enzyme-digested particle-bound strand B, (6) enzyme-digested free strand B, (7) intact strand B, (8) particle-bound strand A, (9) strand A displaced by DTT in the digestion buffer, and (10) 10 bp DNA ladder.

149 strands/particle (corresponds to a surface density of 78.8 pmol/cm^2). This surface coverage is about twice the amount that obtained in the work by Demers and co-workers.[14] We attribute this to the fact that shorter ssDNA used in this study has smaller steric hindrance. In addition, the higher ionic strength condition (500 mM NaCl) used in ssDNA binding may screen the electrostatic repulsion among ssDNA strands more efficiently.

As shown in Figure 3, with the increasing surface coverage of dT-ssDNA, an obvious increase in the digestion efficiency of nAu-bound strands A from 0% to 92% was observed. A similar trend was also found for the digestion of the nonthiol strand A by simply mixing the nonthiol strand A and nAu together prior to the addition of *Eco*RV. The presence of nAu without dT-ssDNA modification (ratio of dT-ssDNA and nAu = 0) results in 0% digestion, even though the target strand A is not bound on nAu. This further confirms that the low digestion efficiency can only be attributed to the presence of bare nAu, which leads to enzyme adsorption on the particles and loss of activity. Again, higher molar ratios of dT-ssDNA to nAu lead to higher surface coverage and substantially improve the digestion efficiency. For both cases, more than 90% digestion efficiency, which is comparable to the digestion efficiency of pure DNA in solution (approximately 95%), can be achieved when the molar ratio between dT-ssDNA and nAu reaches 400:1. At this ratio, the surface of nAu can be considered as sufficiently covered by ssDNA, and therefore the enzyme adsorption is virtually eliminated.

Enzyme Digestion Efficiency of Nanoparticle-Bound DNA. The result of enzyme digestion efficiency of 10 nm nAu-bound DNA mentioned above was obtained from a 12% polyacrylamide gel electrophoresis (PAGE). Figure 4 shows a typical PAGE image of the enzyme-digested and non-enzyme-treated dsDNA (a 500:1 molar ratio of dT-ssDNA to nAu was used in this particular test). It is clearly shown in the figure that both strands A and B, bound on nAu (lanes 2 and 5) or existing as free molecules in the solution (lanes 3 and 6), show exactly the same mobility in the gel after enzyme digestion, which is obviously quicker than the corresponding intact DNA without enzyme treatment (lanes 4 and 7). This shows that the enzyme-cutting site is not shifted by the presence of a bulky nanoparticle, even if the cutting site is located only 18 bases away from the surface of the nAu (strand A). Matching the results shown in Figure 3, the obvious absence of the 80 bases bands in lanes 2 and 5 demonstrates the high efficiency of the enzyme digestion. The digestion efficiency of nAu-bound DNA was found to be above 90% for both strands A and B, which is as high as that of the free DNA digestion (without the presence of nAu) at similar digestion conditions (Table 1). This digestion efficiency

Table 1. Digestion Efficiency of Free DNA and 10 nm nAu-Bound dsDNA by Endonuclease *Eco*RV

	digestion efficiency of free DNA (%)	digestion efficiency of 10 nm nAu-bound DNA (%)
strand A	92.5	92.0
strand B	93.8	92.7

is substantially higher than the previously reported results by other groups, which is approximately 65%.[12] This is most likely due to the low target DNA loading (i.e., strand A or B) on nAu surface in our system, which leads to much less steric hindrance for the enzyme to bind, to move, and to process the target DNA.

It is well known that the gold−thiol (Au−S) linkage, although thermodynamically stable, is kinetically labile and may be displaced by other thiolated compounds. This phenomenon is commonly referred to as "thiol exchange". In our enzyme digestion experiment, the nAu-bound dsDNA may possibly be detached by dithiothreitol (DTT) because DTT, as a common reducing agent, was put in the digestion buffer to prevent possible oxidation of the restriction enzyme. To confirm that the particle-bound dsDNA was not first released by DTT in the digestion buffer before it was digested by *Eco*RV, nAu-bound strand A was incubated at exactly the same digestion condition but without the restriction enzyme. Subsequently, the nAu−strand A conjugates were centrifuged. The supernatant, which contained dsDNA released by DTT, was separated from the pellet, which contained nAu-bound DNA. Finally, pellet was mixed with excess DTT to release all bound strand A for PAGE quantification. As shown in Figure 4, lanes 8−10 correspond to nAu-bound strand A, strand A displaced by the digestion buffer, and 10 bp DNA ladder, respectively. By comparing lanes 8 and 9, it was found that only a trace amount of strand A was released by the digestion buffer (approximately 1%), indicating that the DTT displacement of particle-bound dsDNA was negligible under this digestion condition. This confirms that the low DTT concentration condition adopted in our experiment (1 μM) was tolerable for the particle-bound dsDNA and, at the same time, sufficient to preserve enzyme activity to achieve the high digestion efficiency of the particle-bound dsDNA.

This high enzyme digestion efficiency of nAu-bound DNA was further confirmed using fluorescein-modified dsDNA (FITC strand A, Figure 1). The digestion efficiency was obtained by dividing the fluorescent emission measurement (520 nm) of the *Eco*RV-treated sample by that of the identical sample without enzyme treatment. For the sample without enzyme treatment, the nAu-bound FITC strand A was released from particle by ligand exchange reaction with DTT. Figure 5 shows the typical fluorescent spectrum of the FITC strand A with and without enzyme treatment. Based on the measurement, the digestion efficiency of nAu-bound FITC strand A was found to be 91.4%, a result that is consistent with the one obtained from PAGE characterization shown above. Thus, we have shown here an efficient way of controlling the length of nAu-bound DNA (in this case, 18 or 43 bp long) via endonuclease digestion. This enzyme manipulation should find applications in preparing a master copy of nanoparticle−DNA conjugates bearing DNA strands with multiple enzyme-cutting sites. When it is required, the length of the nanoparticle-bound DNA can be adjusted using different endonucleases that cleave DNA at different recognition sites.

Effect of Ionic Strength on dT-ssDNA Surface Coverage on nAu and Enzyme Digestion Efficiency. When the same DNA conjugation and enzyme digestion conditions were applied for smaller nAu of 7 nm diameter, it was found that the digestion

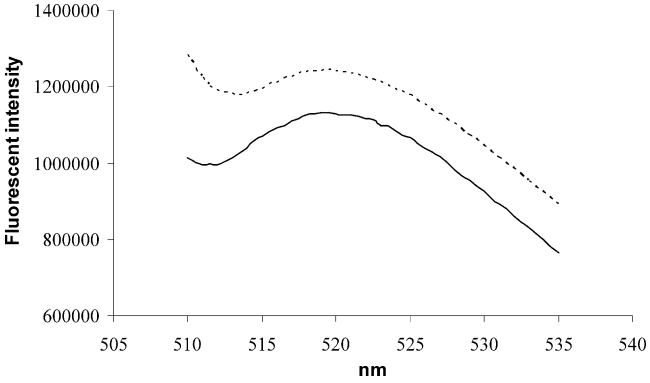

Figure 5. Emission spectrum of FITC strand A used in enzyme digestion efficiency study. Enzyme-digested nAu-bound FITC strand A (−); nAu-bound FITC strand A without enzyme treatment (- - -).

Table 2. dT-ssDNA Surface Coverage on 7 nm nAu under Different NaCl Concentrations and Digestion Efficiencies of Particle-Bound dsDNA by Endonuclease *Eco*RV

NaCl concentration (mol/L)	dT-ssDNA surface coverage on nAu[a] number of strands/nAu	pmol/cm^2	enzyme digestion efficiency (%)	
0.5	62	66.9	strand A	74.4
			strand B	78.7
1.0	69	74.4	strand A	83.7
			strand B	84.2
1.5	82	88.4	strand A	94.0
			strand B	96.3

[a] Determined from fluorescent study using FITC-labeled dT-ssDNA and reported in both units, number of strands/nAu and pmol/cm^2.

efficiencies of particle-bound strand A and strand B drop to 74.4% and 78.7%, respectively. This can be attributed to a lower dT-ssDNA surface coverage on smaller nanoparticles, which leads to a higher possibility that the enzyme adsorbs on the bare gold surface and, therefore, reduces the digestion efficiency. This lower surface coverage of dT-ssDNA on smaller particle was not unexpected. Because of the anionic nature of the nAu surface and DNA, the protocol for dT-ssDNA saturation on nAu requires a gradual increase in NaCl concentration to screen the electrostatic repulsion between the nAu and ssDNA, which was first reported by Mirkin's group.[20] The 7 nm particles have a higher surface charge density than the 10 nm particles, so the 500 mM NaCl concentration, which is sufficient for dT-ssDNA saturation for 10 nm nAu, may not be enough to screen the charge repulsion between 7 nm nAu and dT-ssDNA, resulting in a lower dT-ssDNA surface coverage. Because electrostatic interaction is strongly dependent on the ionic strength of the medium, under higher ionic strength conditions, the charged dT-ssDNA and nAu are expected to be better electrostatically shielded, thus allowing higher surface coverage of dT-ssDNA on nAu. To determine the effect of ionic strength condition on the enzyme digestion of nAu-bound dsDNA, we studied the surface coverage of FITC dT-ssDNA on 7 nm nAu and enzyme digestion efficiency as a function of NaCl concentration used in ssDNA conjugation to nAu. The fluorescent study shows that the dT-ssDNA surface coverage increases with the increasing NaCl concentration (Table 2). It can clearly be seen from the data that higher ionic strength screens the electrostatic repulsion between nAu and dT-ssDNA more efficiently and results in more densely packed ssDNA on nAu surface. This leads to the higher digestion efficiency of particle-bound DNA. Specifically, a 1.5 M NaCl results in 82 dT-ssDNA/nAu (corresponding to

a surface coverage of 88.4 pmol/cm^2) on 7 nm nAu, as well as 94.0% and 96.3% digestion of particle-bound strand A and strand B, respectively. This result is comparable to the one obtained with 10 nm nAu. Thus, besides using expensive dT-ssDNA to increase the surface coverage of ssDNA by increasing the molar ratio of dT-ssDNA to nAu, one can adopt an alternative strategy to increase ssDNA coverage using a high concentration of NaCl to achieve the same degree of high enzyme digestion of particle-bound DNA subsequently. Finally, it is worth mentioning that the labeling of FITC at the 3′ end of the dT-ssDNA may pose some degree of steric hindrance, but, after searching through different fluorophores available for commercial labeling, we found that the molecular sizes of other fluorophores are no better than FITC and thus FITC labeling was adopted in this study.

Conclusions

In this work, we demonstrated the feasibility of enzymatic manipulation of gold nanoparticle-bound dsDNA by restriction endonuclease. We found that the 5-base ssDNA surface coverage on nanoparticles is the key factor that affects the digestion efficiency. Enzyme digestion efficiency can be greatly improved by increasing ssDNA surface coverage on nanoparticles, a process that can be facilitated using high ionic strength conditions. Quantitative study shows that digestion efficiency of particle-bound DNA as high as 90+%, which is similar to free DNA digestion, can be achieved under optimal conditions. Although restriction endonuclease and gold nanoparticles are used in this work, the above results are expected to be applicable to other enzyme reactions (ligation or polymerization) with different kinds of nanoparticles (metallic, semiconductor, or magnetic).

Acknowledgment. We would like to thank the National University of Singapore for providing the doctoral scholarship for W.J.Q. and the research funding (grant R279-000-125-112) for this work.

References and Notes

(1) Sonnichsen, C.; Reinhard, B. M.; Liphard, J.; Alivisatos, A. P. *Nat. Biotechnol.* **2005**, *23*, 741−745. Storhoff, J. J.; Lucas, A. D.; Garimella, V.; Bao, Y. P.; Muller, U. R. *Nat. Biotechnol.* **2004**, *22*, 883−887. Li, H. X.; Rothberg, L. *Proc. Natl. Acad. Sci. U.S.A.* **2004**, *101*, 14036−14039. Lee, T. M. H.; Li, L. L.; Hsing, I. M. *Langmuir* **2003**, *19*, 4338−4343. Nam, J. M.; Thaxton, C. S.; Mirkin, C. A. *Science* **2003**, *301*, 1884−1886. Cao, Y. W. C.; Jin, R. C.; Mirkin, C. A. *Science* **2002**, *297*, 1536−1540. Bailey, R. C.; Nam, J. M.; Mirkin, C. A.; Hupp, J. T. *J. Am. Chem. Soc.* **2003**, *125*, 13541−13547. Georganopoulou, D. G.; Chang, L.; Nam, J. M.; Thaxton, C. S.; Mufson, E. J.; Klein, W. L.; Mirkin, C. A. *Proc. Natl. Acad. Sci. U.S.A.* **2005**, *102*, 2273−2276. Zou, B.; Ceyhan, B.; Simon, U.; Niemeyer, C. M. *Adv. Mater.* **2005**, *17*, 1643−1647. Claridge, S. A.; Goh, S. L.; Frechet, J. M. J.; Williams, S. C.; Micheel, C. M.; Alivisatos, A. P. *Chem. Mater.* **2005**, *17*, 1628−1635. Haberzettl, C. A. *Nanotechnology* **2002**, *13*, 9−13. Jain, K. K. *Expert Rev. Mol. Diagn.* **2003**, *3*, 153−161.

(2) Niemeyer, C. M.; Ceyhan, B. *Angew. Chem., Int. Ed.* **2001**, *40*, 3685−3688. Mbindyo, J. K. N.; Reiss, B. D.; Martin, B. R.; Keating, C. D.; Natan, M. J.; Mallouk, T. E. *Adv. Mater.* **2001**, *13*, 249−254. Loweth, C. J.; Caldwell, W. B.; Peng, X. G.; Alivisatos, A. P.; Schultz, P. G. *Angew. Chem., Int. Ed.* **1999**, *38*, 1808−1812. Hu, J.; Zhang, Y.; Gao, H. B.; Li, M. Q.; Hartmann, U. *Nano Lett.* **2002**, *2*, 55−57.

(3) Maxwell, D. J.; Taylor, J. R.; Nie, S. M. *J. Am. Chem. Soc.* **2002**, *124*, 9606−9612.

(4) Murphy, D.; Eritja, R.; Redmond, G. *Nucleic Acids Res.* **2004**, *32*, e65. Huber, M.; Wei, T. F.; Muller, U. R.; Lefebvre, P. A.; Marla, S. S.; Bao, Y. P. *Nucleic Acids Res.* **2004**, *32*, e137. Sato, K.; Hosokawa, K.; Maeda, M. *Nucleic Acids Res.* **2005**, *33*, e4. Bao, Y. P.; Huber, M.; Wei, T. F.; Marla, S. S.; Storhoff, J. J.; Muller, U. R. *Nucleic Acids Res.* **2005**, *33*, e15. Li, J.; Chu, X.; Liu, Y.; Jiang, J.-H.; He, Z.; Zhang, Z.; Shen, G.; Yu, R.-Q. *Nucleic Acids Res.* **2005**, *33*, e168. Huh, Y. M.; Jun, Y. W.; Song, H. T.; Kim, S.; Choi, J. S.; Lee, J. H.; Yoon, S.; Kim, K. S.; Shin, J. S.; Suh, J. S.; Cheon, J. *J. Am. Chem. Soc.* **2005**, *127*, 12387−12391. Wang, Z. X.; Lee, J.; Cossins, A. R.; Brust, M. *Anal. Chem.* **2005**, *77*, 5770−5774.

(5) Grimm, J.; Perez, J. M.; Josephson, L.; Weissleder, R. *Cancer Res.* **2004**, *64*, 639−643. Chah, S.; Hammond, M. R.; Zare, R. N. *Chem. Biol.* **2005**, *12*, 323−328. Haes, A. J.; Hall, W. P.; Chang, L.; Klein, W. L.; Van Duyne, R. P. *Nano Lett.* **2004**, *4*, 1029−1034.

(6) Hamad-Schifferli, K.; Schwartz, J. J.; Santos, A. T.; Zhang, S. G.; Jacobson, J. M. *Nature* **2002**, *415*, 152−155. Niemeyer, C. M.; Adler, M.; Lenhert, S.; Gao, S.; Fuchs, H.; Chi, L. F. *ChemBioChem* **2001**, *2*, 260−264. Hazarika, P.; Ceyhan, B.; Niemeyer, C. M. *Angew. Chem., Int. Ed.* **2004**, *43*, 6469−6471.

(7) Niemeyer, C. M.; Mirkin, C. A. *Nanobiotechnology: concepts, applications and perspectives*; John Wiley & Sons: Weinheim, 2004.

(8) Pingoud, A.; Jeltsch, A. *Eur. J. Biochem.* **1997**, *246*, 1−22.

(9) He, L.; Musick, M. D.; Nicewarner, S. R.; Salinas, F. G.; Benkovic, S. J.; Natan, M. J.; Keating, C. D. *J. Am. Chem. Soc.* **2000**, *122*, 9071−9077.

(10) Yun, C. S.; Khitrov, G. A.; Vergona, D. E.; Reich, N. O.; Strouse, G. F. *J. Am. Chem. Soc.* **2002**, *124*, 7644−7645.

(11) Kanaras, A. G.; Wang, Z. X.; Bates, A. D.; Cosstick, R.; Brust, M. *Angew. Chem., Int. Ed.* **2003**, *42*, 191−194.

(12) Wang, Z. X.; Kanaras, A. G.; Bates, A. D.; Cosstick, R.; Brust, M. *J. Mater. Chem.* **2004**, *14*, 578−580.

(13) Handley, D. A. *Colloidal Gold: Principles Methods and Applications*; Academic Press: New York, 1989.

(14) Demers, L. M.; Mirkin, C. A.; Mucic, R. C.; Reynolds, R. A.; Letsinger, R. L.; Elghanian, R.; Viswanadham, G. *Anal. Chem.* **2000**, *72*, 5535−5541.

(15) Levicky, R.; Herne, T. M.; Tarlov, M. J.; Satija, S. K. *J. Am. Chem. Soc.* **1998**, *120*, 9787−9792. Swearingen, C. B.; Wernette, D. P.; Cropek, D. M.; Lu, Y.; Sweedler, J. V.; Bohn, P. W. *Anal. Chem.* **2005**, *77*, 442−448.

(16) Storhoff, J. J.; Elghanian, R.; Mirkin, C. A.; Letsinger, R. L. *Langmuir* **2002**, *18*, 6666−6670.

(17) Parak, W. J.; Pellegrino, T.; Micheel, C. M.; Gerion, D.; Williams, S. C.; Alivisatos, A. P. *Nano Lett.* **2003**, *3*, 33−36.

(18) Fischer, N. O.; McIntosh, C. M.; Simard, J. M.; Rotello, V. M. *Proc. Natl. Acad. Sci. U.S.A.* **2002**, *99*, 5018−5023. Verma, A.; Simard, J. M.; Rotello, V. M. *Langmuir* **2004**, *20*, 4178−4181.

(19) Dubertret, B.; Calame, M.; Libchaber, A. J. *Nat. Biotechnol.* **2001**, *19*, 365−370. Li, H. X.; Rothberg, L. J. *Anal. Chem.* **2004**, *76*, 5414−5417.

(20) Storhoff, J. J.; Elghanian, R.; Mucic, R. C.; Mirkin, C. A.; Letsinger, R. L. *J. Am. Chem. Soc.* **1998**, *120*, 1959−1964.

BM060517O